

# Wood-steel structure for vehicle restraint systems

C. Goubel<sup>1ab</sup>, M. Massenzio<sup>a</sup>, S. Rone<sup>1a</sup>

a : Université de Lyon, F - 69622, Lyon, France ; IFSTTAR, UMR\_T9406, LBMC, Bron ; Université Lyon 1, Villeurbanne.

b : Laboratoire INRETS Equipements de la Route (LIER SA) - Lyon Saint Exupéry Aéroport, France

## Summary:

Certain roadside safety barriers are structures made of steel and wood. This kind of structure is currently in fashion in location where the safety equipments need to be discreet (mountains, countryside).

In Europe, to be installed on the roadside, the vehicle restraint systems have to pass two crash tests, as defined in the European standard EN1317.

Our aim is to develop a dynamic model of the multi material structure in order to understand and optimize the safety barriers i.e. to define the best association of the mechanical properties of both materials.

The first part of this paper concerns three point bending experimental tests at different energy levels. These laboratory tests were used as a basis for the evaluation of a material constitutive law.

Then, a numerical parametric study which takes into account the variation of moisture content and temperature, as observed in the experiment, will be exposed.

After that, a model of a roadside safety barrier and a procedure based on variation of failure modes analysis will be presented in order to correlate the numerical model to the real crash test results.

Finally, a parametric study, concerning wood mechanical properties, will be performed in order to check the effect of this variation on the device performances.

## Keywords:

Road Equipment Safety, Crash tests, Finite Element model, Wood-steel structure, LS-Dyna

## Notation:

|            |                             |
|------------|-----------------------------|
| <i>ASI</i> | Acceleration Severity Index |
| <i>W</i>   | Working Width               |
| $\mu$      | Mean value                  |
| $\sigma$   | Standard deviation          |
| <i>CV</i>  | coefficient of variation    |

# WOOD-STEEL STRUCTURE FOR ROADSIDE SAFETY BARRIER

## Context

European road restraint systems are evaluated according to the European standard EN1317 [1]. Generally, two crash tests are needed, one light vehicle - 900kg - used to assess the severity of the device and one heavy vehicle, depending on the restraint level - from 1100 kg up to 38 tonnes - to assess the restraining capacity and the working width (see Figure 1). For instance, for an N2 restraint level – “normal level” in which most of the steel-wood restraint systems can be found - the heavy vehicle is a 1500 kg car at 20° and 110 km/h.

The ASI index is intended to give a measurement of the severity of the deceleration for a person within a vehicle during an impact with a road restraint system. It’s a non dimensional quantity computed using the following equation [1]:

$$ASI = \max \left( \sqrt{\left(\frac{\bar{a}_x(t)}{12}\right)^2 + \left(\frac{\bar{a}_y(t)}{9}\right)^2 + \left(\frac{\bar{a}_z(t)}{10}\right)^2} \right) \quad [1]$$

Where

$$\bar{a}_{x,y,z} = \frac{1}{\delta} \int_t^{t+\delta} a_{x,y,z} dt \quad [2]$$

Equation [2] represents the 3 components of the vehicle acceleration averaged over a moving time interval  $\delta=0.05s$ .

The Figure 1 introduces the Working width which is the distance between the traffic face of the restraint system and the maximum dynamic lateral position of any major part of the system.

The Figure 1 also introduces the Dynamic deflexion ( $D_m$ ) which is the maximum lateral dynamic displacement of the side facing the traffic of the restraint system

More details of these measurements could be find in the European standard EN1317 [2].

It is commonly accepted that steel-wood devices have an aesthetic interest and are most used in places where infrastructure has to be discrete and well integrated into the landscape (mountains, countryside,). Nevertheless, if one focus on the N2 level devices, it’s interesting to notice that significant differences exist between the different kinds of device as illustrated in the Figure 2.

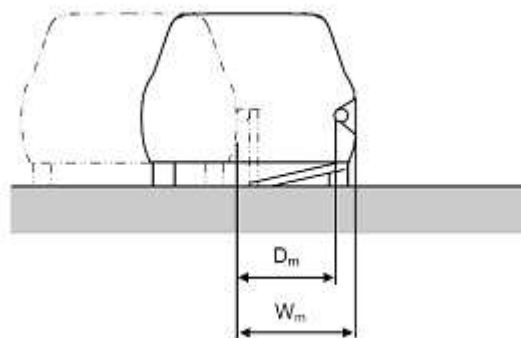


Figure 1: Working Width and dynamic deflection definition

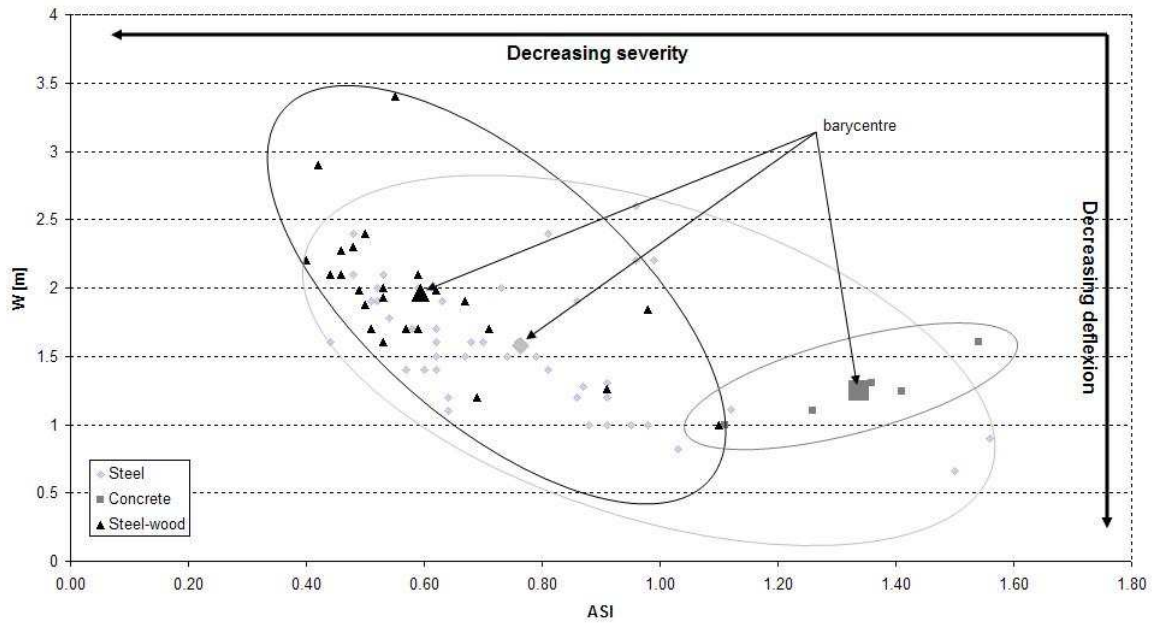


Figure 2: N2 device statistics from LIER test database

It's obvious that concrete devices (very few results presented as most of concrete devices are tested to a higher containment level) are characterized by quite high severity index values on one hand, but on the other hand, by low values of deflexion.

It's certain that there is less difference between steel products and wood-steel products. It's seems that, on average, products including wood are generally less aggressive (lower value for severity indices) but with higher working width which is not necessarily a good sales argument.

The aim of our work is to better understand the use of wood in roadside safety barriers and, hopefully to optimize it and to overpass the aesthetic point of view.

To fulfil this objective, experimental laboratory tests were set-up in order to assess the accuracy of a multi material numerical model.

## THREE POINT BENDING EXPERIMENTAL TESTS

Wood structures responses under dynamic loading have not been much investigated. A large amount of data concerning elastic characteristics is available in the literature [3].

In order to enhance the accuracy of our finite element model, experimental tests are required. The idea is to have a simple test configuration with energy level of the same order of magnitude as those observed during the real crash tests with wooden sample with the same geometrical and mechanical characteristics.

### Tests set-up

Tests were performed at INRETS catapult with a 2 tonnes bogie. The different elements of structure of 2 meters length were simply supported in front of two rigidly fixed concrete blocs with a distance of 1.7m between supports.

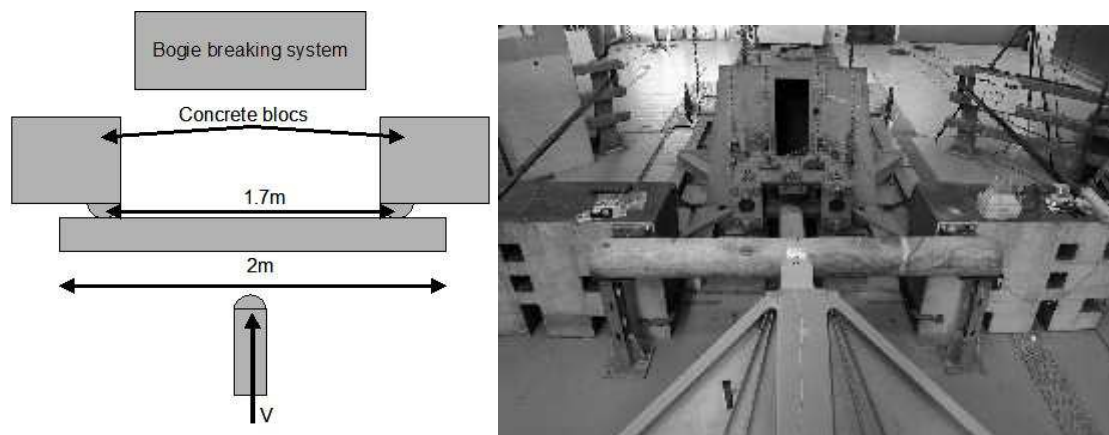


Figure 3: Tests set-up

During the test, acceleration data of the bogie and forces were recorded

### Test matrix and samples

We decided to test two kinds of structure, wood and an assembly of steel and wood (as illustrated in Figure 4). Three levels of energy were chosen and each configuration was tested three times to assess the repeatability of the process.

A total of 18 tests were performed following the test matrix presented in Table 1 below:

| Speed \ Structure | Wood    | Steel-Wood |
|-------------------|---------|------------|
| 5 kmph            | 3 tests | 3 tests    |
| 10 kmph           | 3 tests | 3 tests    |
| 20 kmph           | 3 tests | 3 tests    |

Table 1: Test matrix

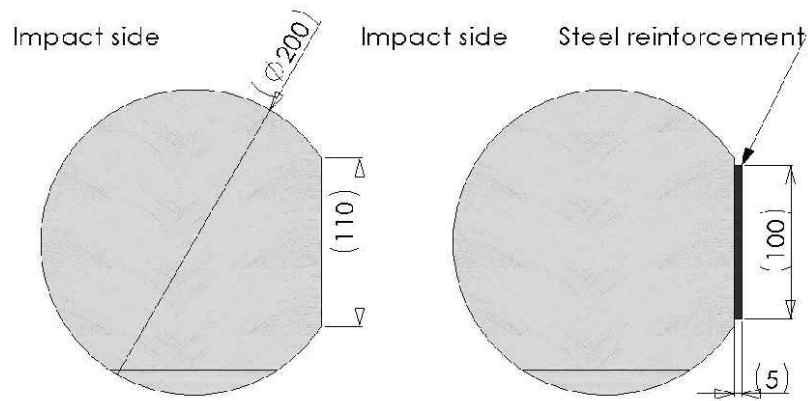


Figure 4 left: wood sample – right: steel-wood sample

A total of 20 wood beams were received from a roadside safety system producer. The samples were supposed to be in regular conditions of use for roadside safety purpose. For steel-wood samples tests, a 5mm thickness steel reinforcement was fixed to the wood beam by the use of two M16 bolts. Special care was taken regarding mass and moisture content of each sample. The moisture content was recorded at 3 points along the wood sample.

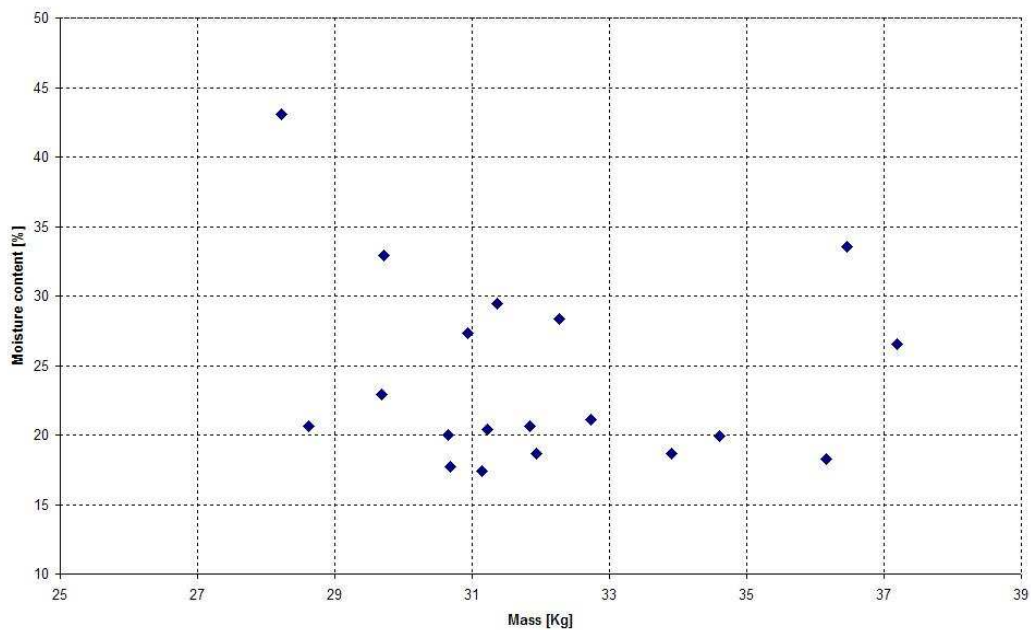


Figure 5: Moisture content measurement

Figure 5 clearly illustrates that no correlation was found between moisture content measurements and the total mass of the sample. The dispersion in mass and moisture content give an indication of the heterogeneity of the wood material.

## Results

During the test, acceleration data for the bogie was recorded as well as forces (via load cells placed between supports and concrete units) with a data acquisition system at 10 000 Hz. The test area was also covered by two high speed cameras (1000 fps).

In this paper, only acceleration data are presented and discussed.

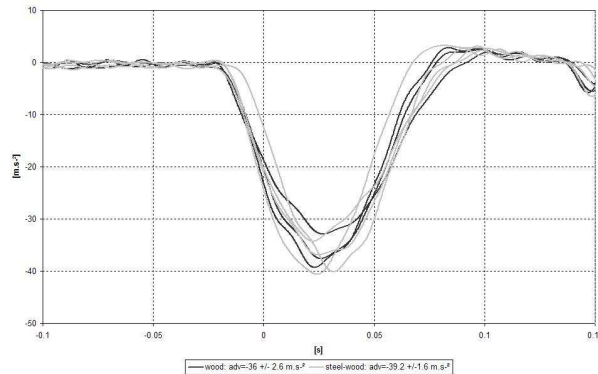


Figure 6: Acceleration of 5 km/h tests

For the lowest level of energy (2 tonnes bogie with an impact speed of 5 km/h), none of the samples failed. The responses of the two different structures are very similar and are characterized by a common single deceleration profile as shown in Figure 6. Even if this test configuration must be considered as being far from the reality of roadside safety system crash testing, it's interesting to notice that, without failure (which must be the case for roadside safety products) there is no significant effect of the steel reinforcement.

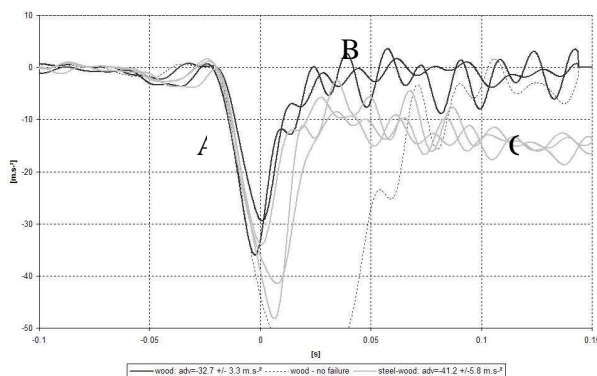


Figure 7: acceleration of 10 km/h tests

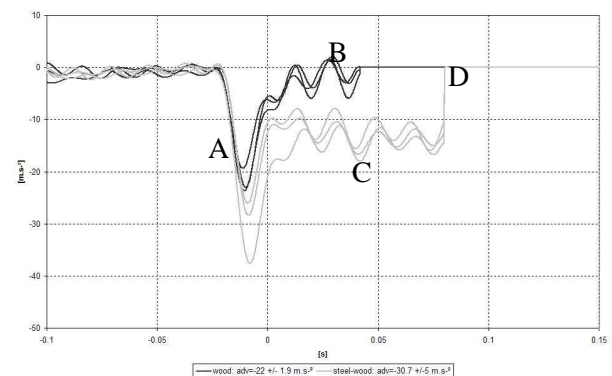


Figure 8: acceleration of 20 km/h tests

At higher level of energy only one sample did not fail (in dashed black line in Figure 7). This result, being very different from the other, is not taken into account either for the calculation of the experimental corridors or for the average deceleration peak value.

The differences between the two kind of structures tested occur after the failure. In Figure 7 & Figure 8, the first deceleration slope (A) is the same for all samples. Wood samples are characterised by a single peak deceleration which leads to failure (B). Steel-wood samples could be identified by higher peaks at later time values and, after failure of the wood part, by a deceleration plateau (C) due to the plastic deformation of the steel reinforcement.

Curves are set to zero (D) to avoid the deceleration profile due to the braking of the bogie.

| Test conditions     |              |      |                  |              |      |                      |              |      |                  |              |      |            |
|---------------------|--------------|------|------------------|--------------|------|----------------------|--------------|------|------------------|--------------|------|------------|
| Speed [km/h]        |              |      | Sample mass [kg] |              |      | Moisture content [%] |              |      | Temperature [°C] |              |      |            |
| target speed [km/h] |              | wood | steel-wood       |              | wood | steel-wood           |              | wood | steel-wood       |              | wood | steel-wood |
| 5                   | $\mu$        | 4.9  | 4.9              | $\mu$        | 31.6 | 39.2                 | $\mu$        | 23.3 | 21.1             | $\mu$        | 24.1 | 25.7       |
|                     | $\sigma$     | 0.1  | 0.2              | $\sigma$     | 1.3  | 0.5                  | $\sigma$     | 7.3  | 4.4              | $\sigma$     | 1.5  | 2.1        |
|                     | $\sigma/\mu$ | 2%   | 4%               | $\sigma/\mu$ | 4%   | 1%                   | $\sigma/\mu$ | 31%  | 21%              | $\sigma/\mu$ | 6%   | 8%         |
| 10                  | $\mu$        | 9.7  | 9.8              | $\mu$        | 33.4 | 43.2                 | $\mu$        | 22.5 | 35.0             | $\mu$        | 23.3 | 25.4       |
|                     | $\sigma$     | 0.0  | 0.0              | $\sigma$     | 2.7  | 1.8                  | $\sigma$     | 2.8  | 14.8             | $\sigma$     | 0.9  | 0.0        |
|                     | $\sigma/\mu$ | 0%   | 0%               | $\sigma/\mu$ | 8%   | 4%                   | $\sigma/\mu$ | 13%  | 42%              | $\sigma/\mu$ | 4%   | 0%         |
| 20                  | $\mu$        | 19.7 | 19.3             | $\mu$        | 28.6 | 41.3                 | $\mu$        | 23.9 | 28.6             | $\mu$        | 21.6 | 25.4       |
|                     | $\sigma$     | 0.1  | 0.3              | $\sigma$     | 0.5  | 2.7                  | $\sigma$     | 6.4  | 10.3             | $\sigma$     | 1.4  | 0.4        |
|                     | $\sigma/\mu$ | 1%   | 1%               | $\sigma/\mu$ | 2%   | 7%                   | $\sigma/\mu$ | 27%  | 36%              | $\sigma/\mu$ | 6%   | 1%         |

| Results             |              |       |            |
|---------------------|--------------|-------|------------|
| target speed [km/h] |              | wood  | steel-wood |
| 5                   | $\mu$        | -36.0 | -39.2      |
|                     | $\sigma$     | 2.6   | 1.6        |
|                     | $\sigma/\mu$ | -7%   | -4%        |
| 10                  | $\mu$        | -32.7 | -41.2      |
|                     | $\sigma$     | 3.3   | 5.8        |
|                     | $\sigma/\mu$ | -10%  | -14%       |
| 20                  | $\mu$        | -22.0 | -30.7      |
|                     | $\sigma$     | 1.9   | 5.0        |
|                     | $\sigma/\mu$ | -9%   | -16%       |

|                          |   |
|--------------------------|---|
| mean value               | $\mu = \frac{\sum X}{N}$                          |
| standard deviation       | $\sigma = \sqrt{\frac{\sum X^2 - N\mu^2}{N - 1}}$ |
| coefficient of variation | $CV = \frac{\sigma}{\mu}$                         |

Table 2: Qualitative analysis

The bogie speed was very well controlled since the mean value of the coefficient of variation for the speed parameter is 1%. For sample mass and room temperature, the mean values of the coefficients of variation are 4% which remains acceptable.

On the contrary, for moisture content, this value reaches 28%. Furthermore, the variation of this parameter is quite well correlated with the variation of the results values. In Table 2, the highest values for variation of moisture content (36% and 42%) could be linked to the highest variation of the deceleration peak value (-16% and -14% respectively).

### THREE POINT BENDING NUMERICAL MODEL

In this section a numerical model of the three point bending experiment will be presented and compared to experimental results. Furthermore, a parametric study will be performed in order to represent the variation of moisture content and temperature as observed in the experiment.

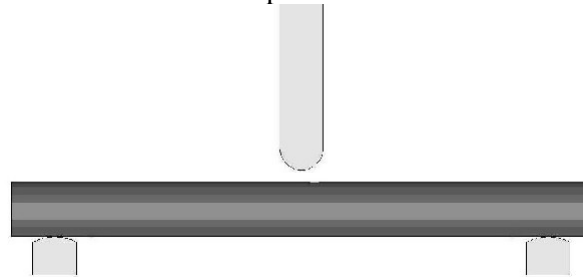


Figure 9: Numerical model

The numerical model contains around 6000 finite elements. The bogie is considered rigid as well as the supports. Initial velocity is applied to the rigid bogie.

The aim is to have a simple model with an element size which could be applicable for a full restraint system modelling (100 meters approximately). Moreover, crash tests against roadside safety barriers usually mean high end times (more than 1s) which lead us to constantly search for a compromise between mesh refining and total number of elements.

For wood modelling, MAT\_WOOD (type 143 available in Ls-Dyna) was used. This model, developed under contract from the FHWA [4], consists in a transversely isotropic material. Our interest is that default material properties for yellow pine are available and temperature and moisture content could be changed (0°C - 10°C - 20°C - 30°C and 0% - 10% - 20% -30% respectively).

A parametric study was performed with “Pine” default properties at 2 temperatures (20°C & 30°C) and two moisture content levels (20% & 30%) which enclose the experimental values of these parameters. Thus, 4 shots were run with Ls-Dyna explicit solver [5,6] and compared to the real test corridor which were constructed by computing the mean value +/- its standard deviation for both structures at each velocity. As an example of mechanical properties variations related to this physical parameter changes, a simple tensile test results are shown in Figure 10 and the corresponding parallel properties are listed in Table 3.

|  |           |           |           |           |
|--|-----------|-----------|-----------|-----------|
| <b>Moisture content [%]</b>            | <b>30</b> | <b>30</b> | <b>20</b> | <b>20</b> |
| <b>Temperature [°C]</b>                | <b>30</b> | <b>20</b> | <b>30</b> | <b>20</b> |
| <b>Parallel Normal Modulus [MPa]</b>   | 10610     | 11428     | 11898     | 12512     |
| <b>Parallel Tensile Strength [MPa]</b> | 34.8      | 40        | 46.7      | 52.3      |

Table 3- Wood mechanical properties variation

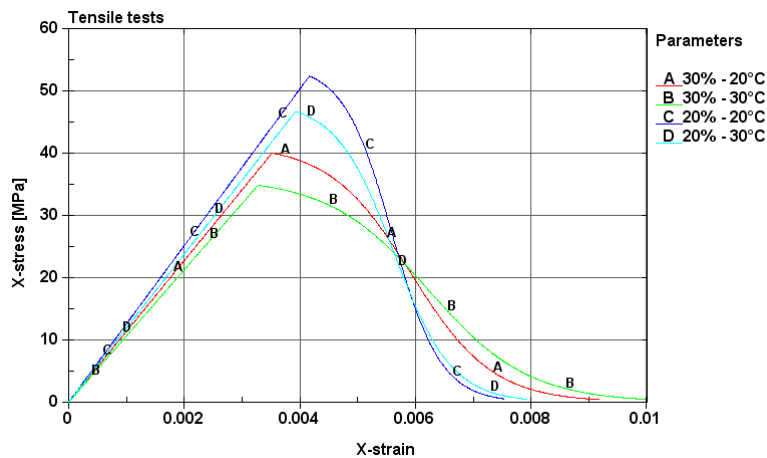


Figure 10 – Wood tensile test

## Results at 5 km/h

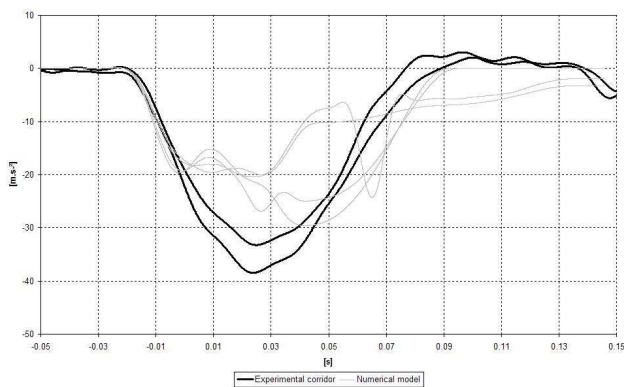


Figure 11: Wood results at 5 km/h

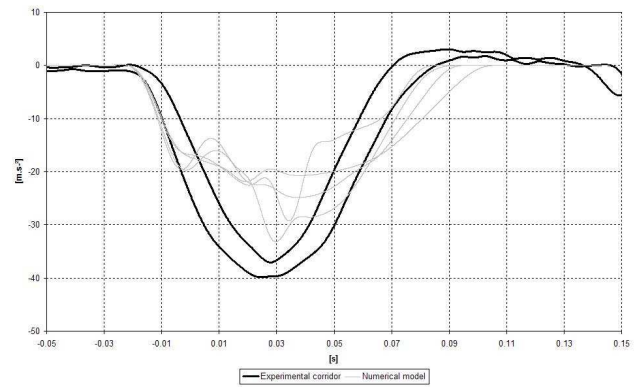


Figure 12: Steel-wood results at 5 km/h

## Results at 10 km/h

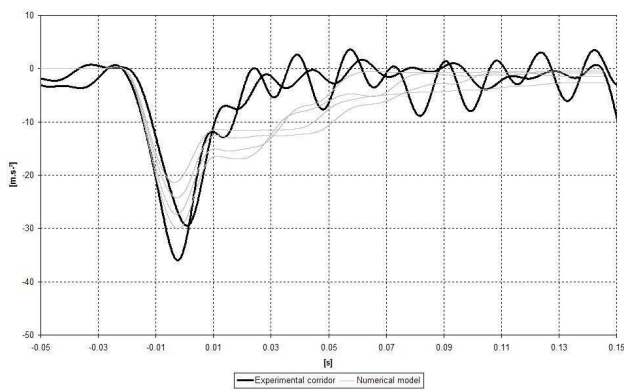


Figure 13: Wood results at 10 km/h

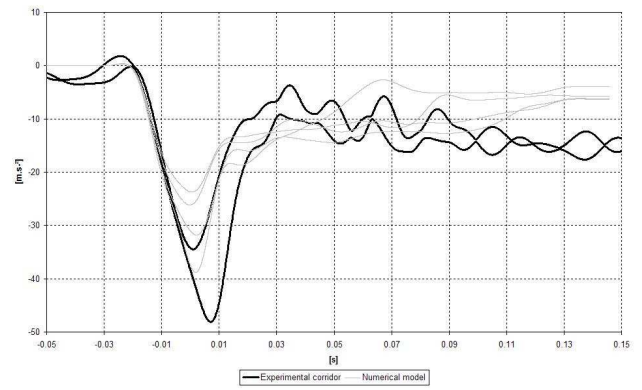


Figure 14: Steel-wood results at 10 km/h

## Results at 20 km/h

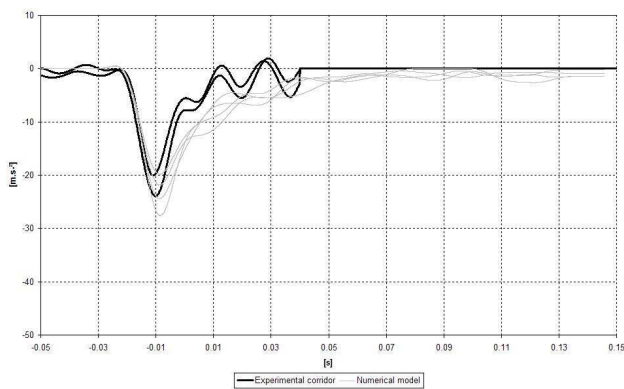


Figure 15: Wood results at 20 km/h

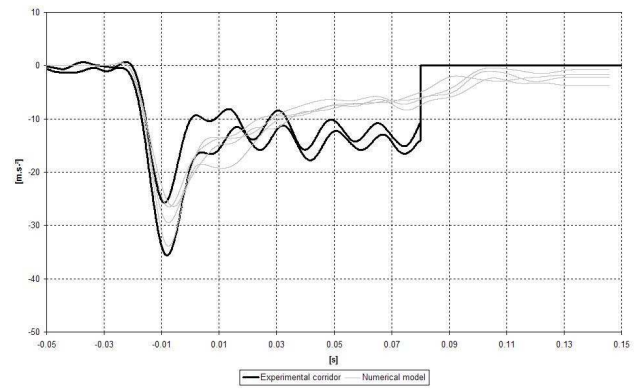


Figure 16: Steel-wood results at 20 km/h

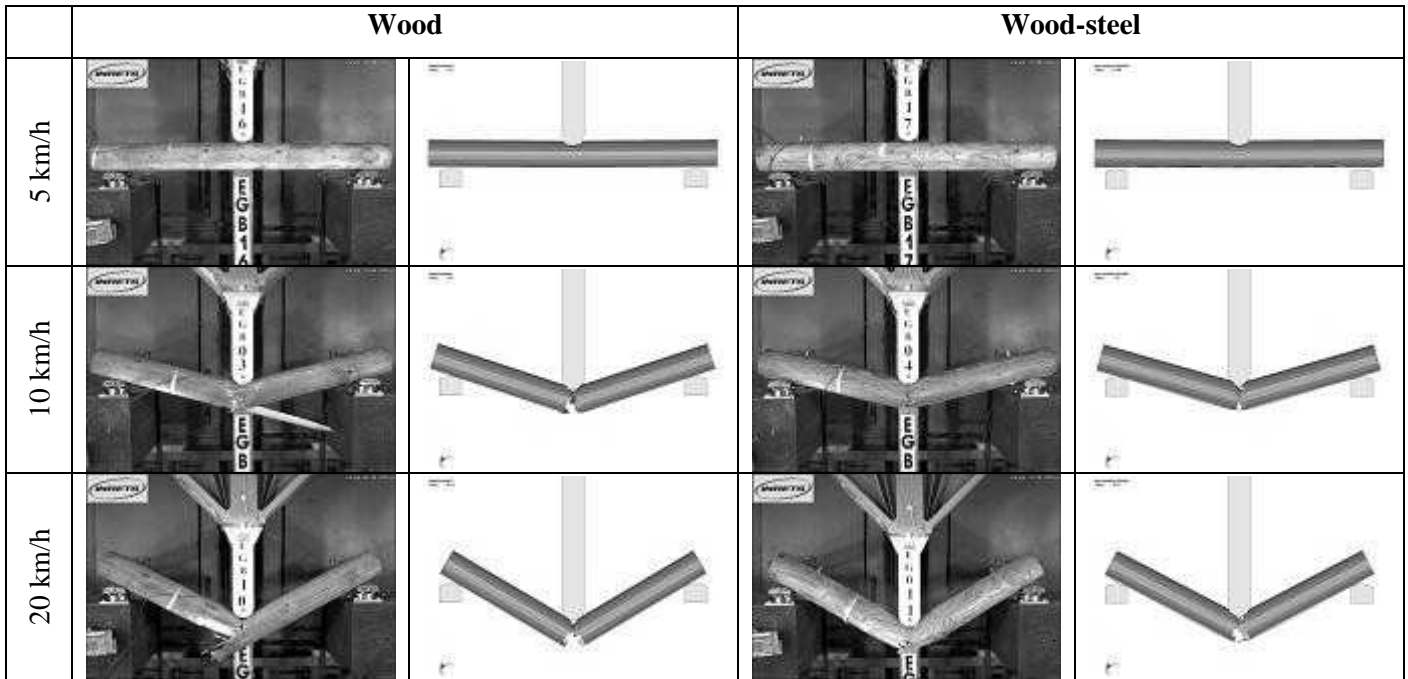


Table 4: Failure modes comparison

| target speed<br>[km/h] |              | Experimental results                    |            | Numerical results                       |            |
|------------------------|--------------|---|------------|---|------------|
|                        |              | Deceleration value [m.s <sup>-2</sup> ] |            | Deceleration value [m.s <sup>-2</sup> ] |            |
|                        |              | wood                                    | steel-wood | wood                                    | steel-wood |
| 5                      | $\mu$        | -36.0                                   | -39.2      | -37.6                                   | -27.3      |
|                        | $\sigma$     | 2.6                                     | 1.6        | 1.6                                     | 4.3        |
|                        | $\sigma/\mu$ | -7%                                     | -4%        | -4%                                     | -16%       |
| 10                     | $\mu$        | -32.7                                   | -41.2      | -25.7                                   | -30.1      |
|                        | $\sigma$     | 3.3                                     | 5.8        | 3.3                                     | 5.8        |
|                        | $\sigma/\mu$ | -10%                                    | -14%       | -13%                                    | -19%       |
| 20                     | $\mu$        | -22.0                                   | -30.7      | -23.4                                   | -29.1      |
|                        | $\sigma$     | 1.9                                     | 5.0        | 2.9                                     | 3.0        |
|                        | $\sigma/\mu$ | -9%                                     | -16%       | -12%                                    | -10%       |

Table 5: Qualitative analysis

First of all, as illustrated in Table 4, our multi-material model perfectly reflects the failure modes observed during the experiments.

Moreover, the results presented in Table 5 indicate that the parametric study performed gives results with a similar dispersion as the experiments.

Concerning acceleration data, Figure 11 and Figure 12 corresponding to test performed at 5 km/h indicate that the curves obtained from the numerical model exit the experimental corridor at an early stage. This could be explained by the local erosion in the contact area that leads to a loss of contact. At this low velocity, the bogie took a long time to find contact again.

At higher velocities, (Figure 13 to Figure 16) this phenomenon is less sensitive due to the fact that erosion mostly occurs on the back side of the beam and drives the failure mode of the structure.

## ROADSIDE BARRIER MODEL

In the previous paragraph a model of a simple steel-wood beam was presented. Its response to a three point bending impact was compared to experimental data.

In this section a model of a complete roadside safety barrier will be presented.

Our aim is to demonstrate the capacity of the model to reproduce a real test configuration (correlation step) and, in a second step, to evaluate the effect of wood mechanical properties, as observed in the three point bending experiment, to the performances of the device.

### Numerical model

A French steel-wood N2-device “solobois” from SOLOSAR has been modelled.

This device is made of a C post every two meters, wood beams, 2 meters length, are connected together by the mean of a spacer at the level of each post. A steel reinforcement (100x5mm) 4 meters length is situated on the middle of the wood beam.

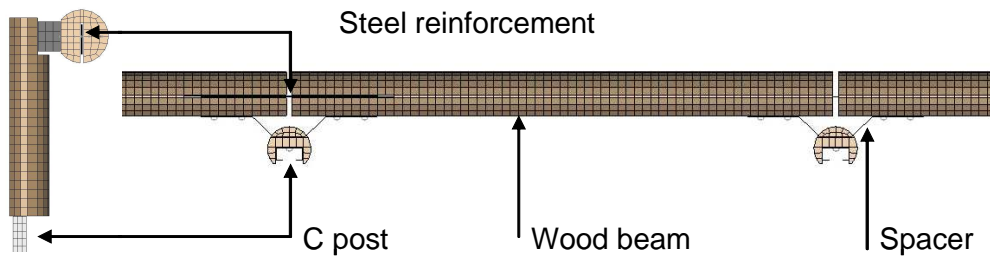


Figure 17 – Model definition

### Correlation

In a crash of vehicle against a Vehicle Restraint System (VRS), a lot of parameters could have an effect to the global behaviour and, thus, to the severity indices and W results.

As the structures are highly solicited (for some component till the failure) the use of standardized data for parameters such as steel yield point could lead to poor correlation. Furthermore, even if the components are checked after crash, uncertainties concerning the real component mechanical properties are remaining.

In the field of roadside safety, when talking about correlation between a simulation and a real test, its frequent to see comparison between one crash configuration (mainly due to the crash test cost) and one simulation.

This point-to-point comparison is unfortunately very poor, as the variation of mechanical properties is quite important and can affect significantly the device performances.

One important issue of this section is to outline a procedure for assessing the intrinsic variability of a VRS and then to compare an experimental result to a cloud of numerical simulations.

The procedure is based on the failure modes analysis. A failure mode is defined by a sequence of events (which is not necessarily failure!) which activates a mechanism in the device.

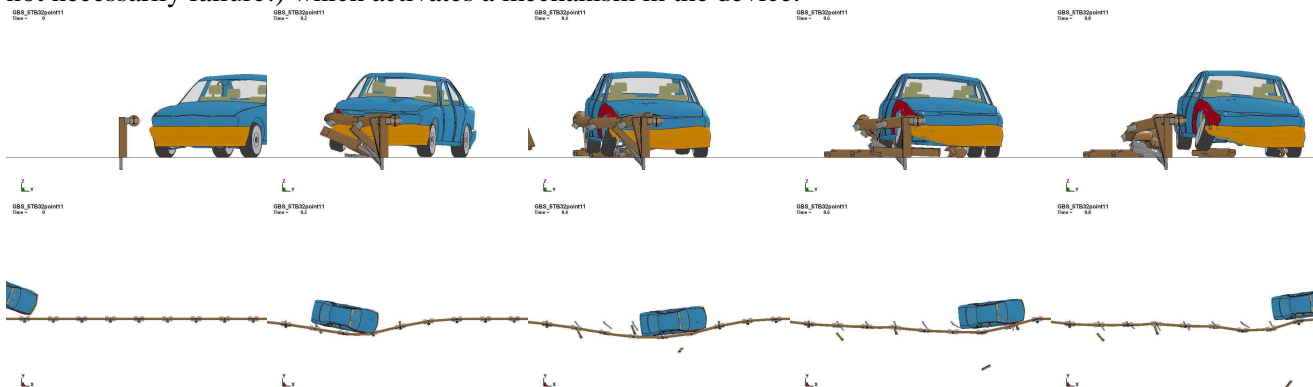


Table 6 Test sequence downstream (above) and top view (below)

Table 6 presents the test sequence of one TB32 simulation.

The analysis of this test sequence leads to the identification of 4 main mechanisms listed in the following Table 7:

| Failure modes  | Illustration | Main parameter          | Average value | Range of variation |
|--|--------------|-------------------------|---------------|--------------------|
| Transfer of the contact force via the steel-wood beam to each connected post |              |                         |               |                    |
| Formation of a plastic hinge at post base                                    |              | Post yield stress       | 300 MPa       | 270 – 330 MPa      |
| Formation of a plastic hinge at each articulation                            |              | Spacer yield stress     | 300 MPa       | 270 – 330 MPa      |
|  |              | Steel rail yield stress | 300 MPa       | 270 – 330 MPa      |
| Post-spacer bolt failure   |              | Bolt force failure      |               | 35 000 – 40 000 N  |

Table 7: Failure modes analysis and parameter variation

In order to obtain a cloud of results, all the identified parameters were defined as design variable in a parametric study. The variation of each parameter was done separately in a factorial design of experiment. The complete design of experiment with the main results is shown in Table 8.

| Shot_ID          | Rail yield [Mpa] | Post yield [Mpa] | Spacer yield [Mpa] | Bolt failure [N] | W [m]       | ASI [NU]    | THIV [km/h]  |
|------------------|------------------|------------------|--------------------|------------------|-------------|-------------|--------------|
| Shot_01          | 270              | 330              | 330                | 40 000           | 1.39        | 0.61        | 24.24        |
| Shot_02          | 270              | 330              | 330                | 35 000           | 1.42        | 0.57        | 23.02        |
| Shot_03          | 270              | 330              | 270                | 35 000           | 1.42        | 0.62        | 24.15        |
| Shot_04          | 270              | 270              | 330                | 40 000           | 1.41        | 0.58        | 23.19        |
| Shot_05          | 270              | 270              | 270                | 35 000           | 1.50        | 0.59        | 23.27        |
| Shot_06          | 270              | 270              | 330                | 35 000           | 1.50        | 0.54        | 21.99        |
| Shot_07          | 270              | 270              | 270                | 40 000           | 1.50        | 0.60        | 23.31        |
| Shot_08          | 330              | 270              | 270                | 40 000           | 1.49        | 0.54        | 22.01        |
| Shot_09          | 330              | 270              | 270                | 35 000           | 1.51        | 0.58        | 23.77        |
| Shot_10          | 270              | 330              | 270                | 40 000           | 1.51        | 0.56        | 22.77        |
| Shot_11          | 330              | 270              | 330                | 40 000           | 1.49        | 0.60        | 23.85        |
| Shot_12          | 330              | 330              | 270                | 40 000           | 1.49        | 0.55        | 22.63        |
| Shot_13          | 330              | 330              | 330                | 40 000           | 1.59        | 0.57        | 22.85        |
| Shot_14          | 330              | 330              | 330                | 35 000           | 1.59        | 0.51        | 21.55        |
| Shot_15          | 330              | 270              | 330                | 35 000           | 1.59        | 0.56        | 22.78        |
| Shot_16          | 330              | 330              | 270                | 35 000           | 1.62        | 0.51        | 21.70        |
| <b>Real test</b> | <b>≥ 235</b>     | <b>≥ 235</b>     | <b>≥ 235</b>       | <b>≥ 33 700</b>  | <b>1.69</b> | <b>0.57</b> | <b>21.80</b> |

Table 8: Design of experiment

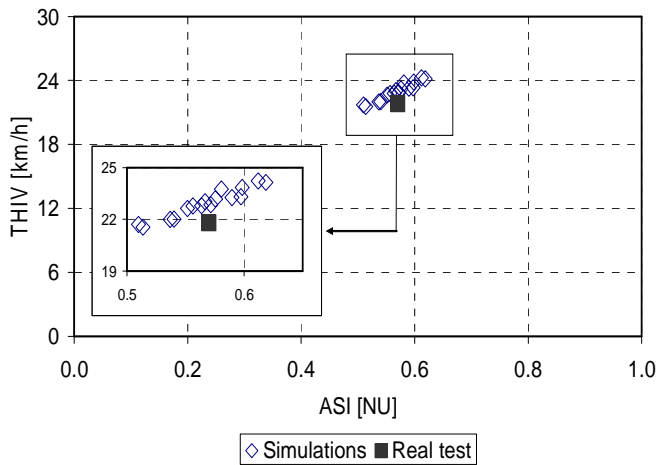


Figure 18: THIV as a function of ASI

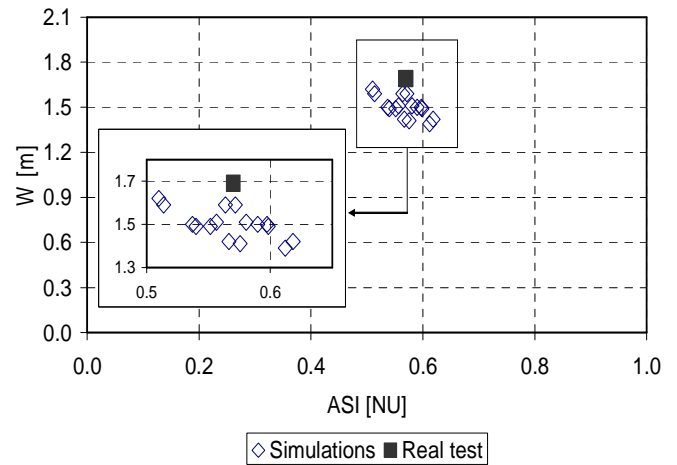


Figure 19: W as a function of ASI

From the global results and from the scatters plots presented in *Figure 18* and *Figure 19*, one can consider that the design of experiment performed enclosed the results of the real test in terms of severity indices.

On the contrary a noticeable difference appears in terms of W. This difference may be due to several reasons:

If one considers that the parametric study performed enclosed the real parameters values, it should indicate that the model is stiffer than the real device. This could be solved, by example, by removing the boundary condition applied at each extremity of the device.

On the contrary, if one considers that the parametric may not enclose the real parameters value, an extension of the variation of post and beam yield stress which are, in our case, the more sensitive parameters concerning W results, must allow to find a better agreement.

Those results very well illustrate the interest of a parametric approach in order to provide a range of possible results which is more relevant than one result based on one parameters set. Even if the numerical model is determinist, its actual input parameters are defined by ranges. One can understand that the material characterization of each device component can't be realized (even more in real life use).

In the CEN TC226/WG1/TG1/CM-E group (Computational Mechanics Europe) the actual position concerning a model response comparison with respect to a real crash test, is to compare velocity components in the global (barrier) reference frame. After rotation of the acceleration data recorded in the vehicle frame thanks to rotation velocity records, the integration gives two component of vehicle velocity in the global (barrier) frame.

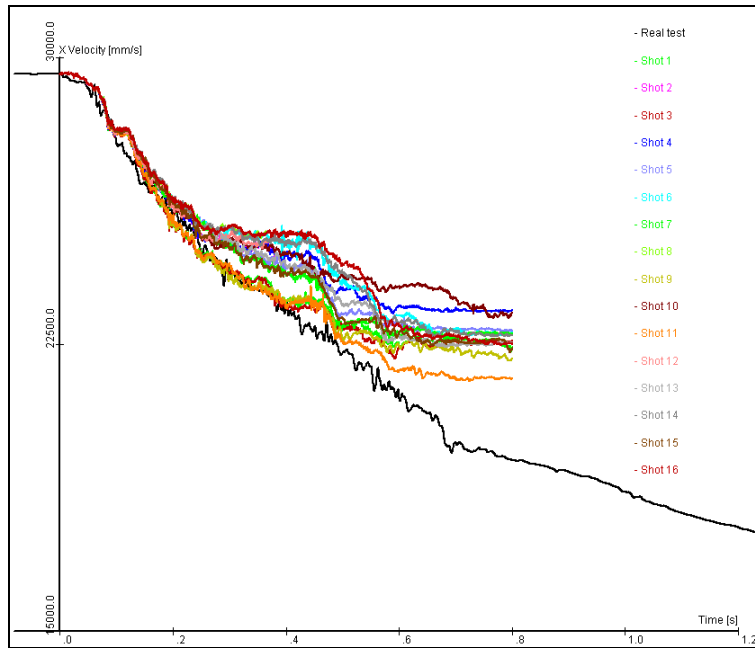


Figure 20: X Velocity components for steel DOE

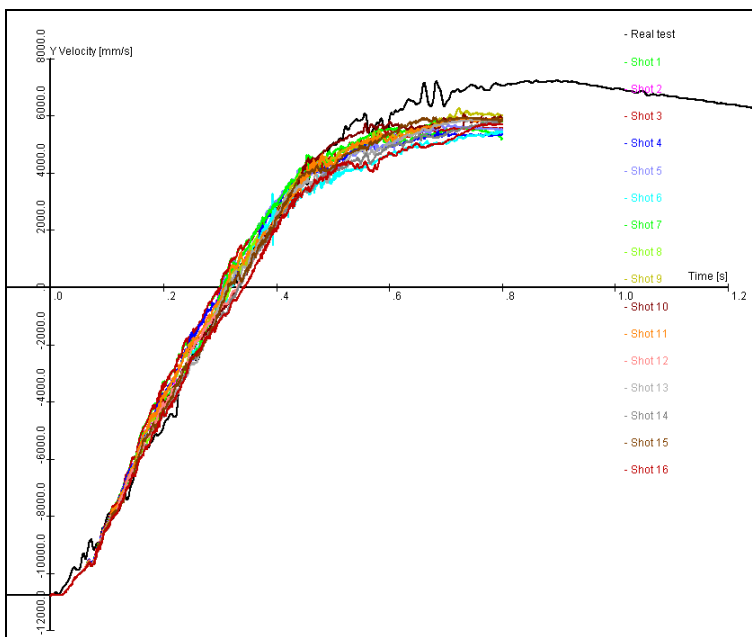


Figure 21: Y Velocity components for steel DOE

| Shot_ID | YvelError | XvelError | Moy(X,Y)Error |
|---------|-----------|-----------|---------------|
| Shot_12 | 403.0     | 390.8     | 396.9         |
| Shot_08 | 361.4     | 447.9     | 404.7         |
| Shot_02 | 472.3     | 420.8     | 446.5         |
| Shot_11 | 671.3     | 679.6     | 675.5         |
| Shot_15 | 496.9     | 903.4     | 700.2         |
| Shot_13 | 562.3     | 859.5     | 710.9         |
| Shot_09 | 611.0     | 945.2     | 778.1         |
| Shot_14 | 578.6     | 978.6     | 778.6         |
| Shot_07 | 633.2     | 983.9     | 808.5         |
| Shot_16 | 650.8     | 966.4     | 808.6         |
| Shot_05 | 749.7     | 1011.8    | 880.8         |
| Shot_06 | 823.7     | 1000.5    | 912.1         |
| Shot_10 | 552.1     | 1330.2    | 941.2         |
| Shot_03 | 862.8     | 1034.5    | 948.6         |
| Shot_01 | 902.4     | 1040.1    | 971.3         |
| Shot_04 | 860.4     | 1232.6    | 1046.5        |

Table 9: Quadratic error

Figure 20 and Figure 21 show the velocity components as a function of time. The black lines (up to 1.2s) are the real test velocity components and the simulations defined a corridor obtained with the parametric study

To select the best simulation, the quadratic error for each component and for each shot was computed. The shot obtaining the lowest average value is then considered as the best one. The results obtained are summed-up in the Table 9 in which red lines concerns the shots without “normal termination” for which the termination time is shorter and the error is necessarily lower. The corresponding shots have been removed for the analysis.

The parameters of the shot 11 have been selected as the best set of parameters to represent the behaviour observed in the real test.

## Wood Mechanical properties variation

Starting from the set of parameter obtained in the correlation step, a second design of experiment concerning the wood variability – as defined in the three point bending test – has been performed. The Table 10 sums-up the parameters and the main results.

| Shot_ID | Moist [%] | Temp [°] | W [m] | ASI [NU] | THIV [km/h] |
|---------|-----------|----------|-------|----------|-------------|
| Shot_02 | 30        | 30       | 1.48  | 0.58     | 23.02       |
| Shot_05 | 30        | 20       | 1.50  | 0.59     | 23.27       |
| Shot_08 | 20        | 30       | 1.49  | 0.60     | 23.38       |
| Shot_11 | 20        | 20       | 1.50  | 0.59     | 23.34       |

Table 10: Wood properties Design of experiment

The results obtained for this design of experiment are very similar. The conclusion is then that the variation of wood properties observed during the three point bending experiment has a quite low effect regarding barrier performances.

In terms of velocity component, one can observe that the four simulations define a very narrow corridor which confirms that the global behaviour is comparable (Figure 22).

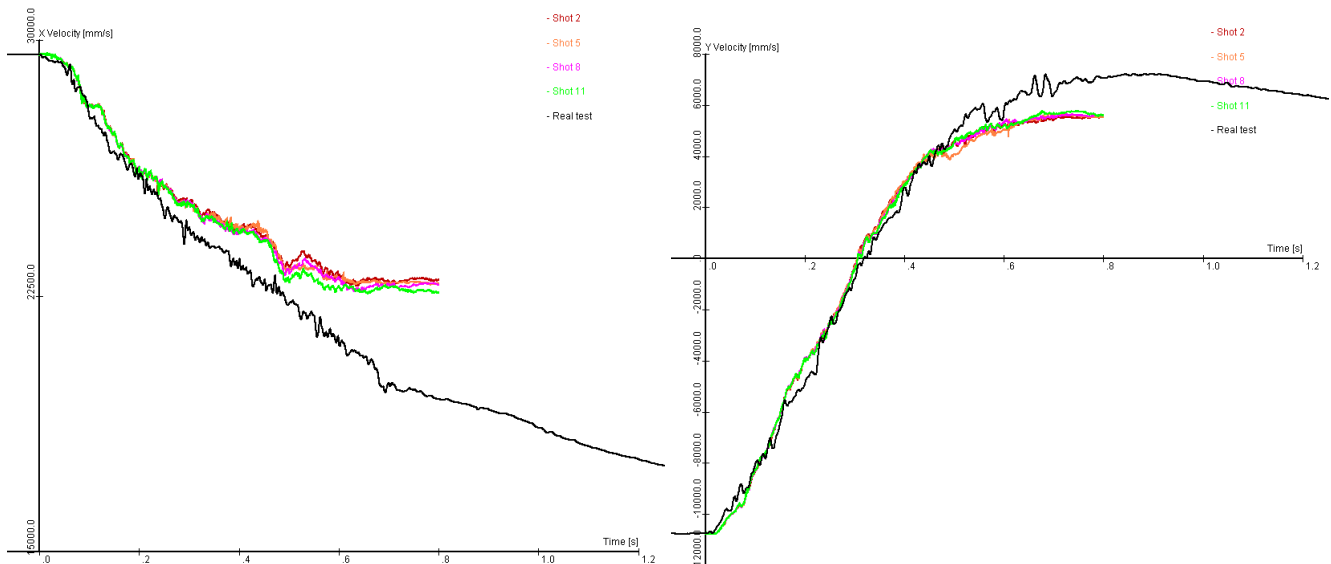


Figure 22: Velocity component for wood DOE - X velocity (left) - Y velocity (right)

Although the mechanical properties of wood were changed about +/- 15% (Table 3) the effect on the behaviour and on the results is very poor.

This reassuring result in terms of safety performances is not necessarily satisfactory in term of structure design. In fact, one interpretation could be that the wood dimensions are oversized.

The next steps of this work will consist on one hand to continue the correlation work and, in the other hand, to initiate the optimization of the steel-wood coupling.

## CONCLUSION

The environment (mainly temperature and moisture content) affects wood mechanical properties. This fact has been highlighted in experimental tests and well represented by a numerical study by the mean of a parametric study.

On the road side, those parameters can vary and can't be controlled. One interest of a numerical model is to take into account those variations in order to obtain a corridor of responses and, thus, to assess their effect to the Vehicle Restraint System performances.

The variation observed in the experiment has been applied to a VRS numerical model in a parametric study. The effect of this variation is very limited towards the device performances as well in terms of severity than deflexion.

The next step of this work will be to optimize the structure in terms of steel-wood coupling in order to obtain better results in terms of W.

## REFERENCES

- [1] CEN, EN 1317-1, "Road restraint system- Part 1: Terminology and general criteria for test methods", 1998
- [2] CEN, EN 1317-2, "Road restraint system – Part 2 : Performances classes, impact test acceptance criteria and test methods for safety barriers", 1998
- [3] D. GUITARD - Mécanique du matériau bois et composites – CEPADUES EDITIONS - 1987
- [4] Y.D. MURRAY, Manual for LS-DYNA Wood Material Model 143, Report No. FHWAHRT- 04-097, Federal Highway Administration, 2004.
- [5] J. O. HALLQUIST, "LS-Dyna Theoretical Manual", Livermore Software Technology Corporation, Livermore 1998
- [6] J. O. HALLQUIST, "LS-Dyna Keyword User's Manual. Version 971", Livermore Software Technology Corporation, Livermore 2007